



# Venus wind map at cloud top level with the MTR/THEMIS visible spectrometer, I: Instrumental performance and first results

Patrick Gaulme<sup>a,\*</sup>, François-Xavier Schmider<sup>b</sup>, Catherine Grec<sup>b</sup>, Arturo López Ariste<sup>c</sup>,  
Thomas Widemann<sup>a</sup>, Bernard Gelly<sup>c</sup>

<sup>a</sup>LESIA, Observatoire de Paris, 5 place J. Janssen, F-92195 Meudon Cedex, France

<sup>b</sup>Laboratoire Fizeau, Université de Nice Sophia-Antipolis, CNRS-Observatoire de la Côte d'Azur, F-06108 Nice Cedex 2, France

<sup>c</sup>THEMIS Observatory, La Laguna, Tenerife, Spain

Received 5 February 2008; received in revised form 29 June 2008; accepted 30 June 2008

Available online 24 July 2008

---

## Abstract

Solar light gets scattered at cloud top level in Venus' atmosphere, in the visible range, which corresponds to the altitude of 67 km. We present Doppler velocity measurements performed with the high resolution spectrometer MTR of the Solar telescope THEMIS (Teide Observatory, Canary Island) on the sodium D2 solar line (5890 Å). Observations lasted only 49 min because of cloudy weather. However, we could assess the instrumental velocity sensitivity, 31 m s<sup>-1</sup> per pixel of 1 arcsec, and give a value of the amplitude of zonal wind at equator at 151 ± 16 m s<sup>-1</sup>.

© 2008 Elsevier Ltd. All rights reserved.

*Keywords:* Venus; Wind; Clouds; Visible; Spectrometry

---

## 1. Introduction

ESA's Venus Express (VEx) space probe has been orbiting around Venus since April 2005. The mission's main goal is a better understanding of the atmospheric circulation, in particular of the wind super-rotation. The key questions regard the meridian circulation at top cloud level, the vertical extension of Hadley cells and the latitudinal dependence of the zonal wind. VEx obtains wind velocity map with cloud tracking and wind vertical profile from thermal wind maps. VEx measurements are limited by three factors. First, because of a very eccentric orbit, i.e. a strong velocity at periastron, VEx is not able to follow the motion of cloud features, at latitude above 20°N. Second, with cloud tracking, the temporal resolution cannot get lower than 1 h. At last, wind measurements are restricted to two levels, corresponding to cloud top, that is to say at 67 km on the day side and 50 km on the night side

(Drossart et al., 2007). That is why, a large ground-based support has been organised around the 2007 Venus' maximum elongation in May–June and early November. The main idea was to get radial velocity measurements with spectrometry, almost simultaneously, in several spectral ranges in order to probe as many levels as possible of the upper atmosphere.

Hereafter, we present spectrometric measurements on the sodium D2 solar line (5890 Å), lead at THEMIS solar telescope (Teide Observatory, Canary Islands), on discretionary time, on November 7th, 2007. The objective of this run was the evaluation of instrumental performance of the MTR spectrometer, for radial velocity measurements on a planetary target. The advantage of MTR/THEMIS spectrometer with respect to point to point echelle-spectrometer measurements is the ability to build velocity maps, using a long slit entrance, greater than planetary diameter, which allows us to scan completely the whole planet with only 15 positions of the slit. Because of cloudy weather, observations lasted only 49 min. However, it is enough to evaluate the signal to noise level and to give an estimate of the zonal wind velocity.

---

\*Corresponding author. Tel.: +33 1 4707 7673; fax: +33 1 4507 7959.  
E-mail address: [Patrick.Gaulme@obspm.fr](mailto:Patrick.Gaulme@obspm.fr) (P. Gaulme).

We present the instrument main properties (Section 2), the data processing (Section 3) and, then, the estimate of the instrumental performance and velocity field (Section 4).

## 2. Instrument main characteristics, observing conditions and expected performance

### 2.1. MTR-THEMIS high resolution spectrometer

THEMIS (Télescope Héliographique pour l'Etude du Magnétisme et des Instabilités Solaires) is a French-Italian solar telescope dedicated to accurate measurement of polarisation of solar spectral lines, with high spatial, spectral and temporal resolutions (Mein and Rayrole, 1985). It is a 90-cm diameter Ritchey–Chrétien telescope. For present observations, it has been operated in the MTR (MulTiRaies) mode (Rayrole and Mein, 1994) which allows spectropolarimetric observations in up to six different spectral domains simultaneously. For radial velocity measurements, the polarimetric analysis was skipped and only spectrometric information is considered. For this test run, we used the existing setup of the instrument and focused on the sodium D2 solar line (5890 Å). It is one of the deeper lines in the optimal spectral domain for MTR detectors, but it is not optimum for Doppler sensitivity. We might search for a better line for future observations.

### 2.2. Observing conditions

Data were acquired on November 7th, 2007 between 13:06:52 and 13:55:34 h (UT). The slit entrance dimension was about  $(0.5 \times 100)$  arcsec. The spectral resolution was about 20 mÅ, while the seeing has been estimated to 1 arcsec. The detector is a  $512 \times 512$  pixels CCD. The spatial dispersion upon the detector was equal to  $0.2 \text{ arcsec pixel}^{-1}$  and the spectral dispersion was equal to  $11.7 \text{ mÅ pixel}^{-1}$ . The exposure time has been set to 10 s, while the readout time was less than 50 ms per exposure. We have considered the latter as negligible.

The planet's diameter was about 21.76 arcsec and the phase angle about  $83.59^\circ$  (Fig. 1 and Table 1), which was close to maximum elongation (on October 27th, 2007). Only 15 scans regularly spaced of about 0.8 arcsec were necessary to map the whole enlightened part of the planet. However, because of bad weather conditions, the scanning schedule got changed and did not work nicely. In particular, no dark field nor flat field was done and the scanning was off. The guiding was manually set on Venus' limb, and the positioning upon the disk slowly drifted along the run. Therefore, the planetary scan was only due to the drift of the planet inside the field of view, which has limited the coverage to 70% of the radius, i.e. an extension of about 8 arcsec along the equator (Fig. 2). Nevertheless, 318 spectra were obtained in the 49-min observation run. Observing conditions were satisfactory during acquisition as illustrated by the stability of the mean intensity of the terrestrial signal (Fig. 3). We could evaluate the instru-

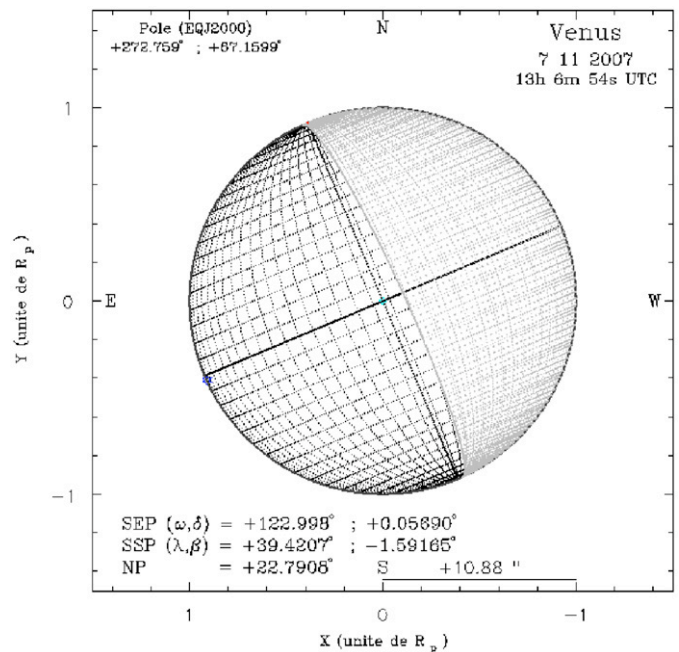


Fig. 1. Venus appearance during observations, on November 7th, 2007 at 13:06:54 h (UTC). The planetary radius is about 10.88 arcsec and the phase angle about  $83.59^\circ$ . SEP and SSP stand for sub-Earth point and sub-solar point.

Table 1

Observation properties of Venus on November 7th, 2008 from Teide Observatory (IMCCE ephemeris database)

Date UTC h m s	RA h m s	December o ' "	Distance ua.	V. Mag	Phase o	Dist dot o
13 6 0.00	11 56 21.86	01 28 42.10	0.77	-4.31	83.58	13.27725
13 56 0.00	11 56 30.16	01 27 57.89	0.77	-4.31	83.56	13.32962

mental performance and estimate qualitatively the velocity range along the scan. The terminator region, where the Sun–Venus Doppler effect is expected to be maximum, is covered by the observation. Expected performance and detailed analysis are presented in next sections.

### 2.3. Theoretical performance

The principle of our observations rests on the measurement of the position of a solar Fraunhofer line (D2, sodium), which gets shifted by Doppler effect after reflection on Venus cloud decks. The radial velocity sensitivity depends on the sodium line thickness and the total amount of photons. First, measured on highly resolved spectrum, the local slope of the D2 sodium line appears to be  $(\delta I/I)_{\text{max}} = 10^{-4}$  per  $\text{m s}^{-1}$  at maximum, or, in average  $\langle \delta I/I \rangle = 0.5 \times 10^{-4}$  per  $\text{m s}^{-1}$  for two 60 mÅ bandwidths at each side of the line (see Fig. 4). Second, knowing that Venus emits almost  $4.8 \times 10^{11} \text{ photons s}^{-1} \text{ m}^{-2} (1000 \text{ Å})^{-1}$  in the visible range on a 187-arcsec square lighted surface, that the telescope's efficient

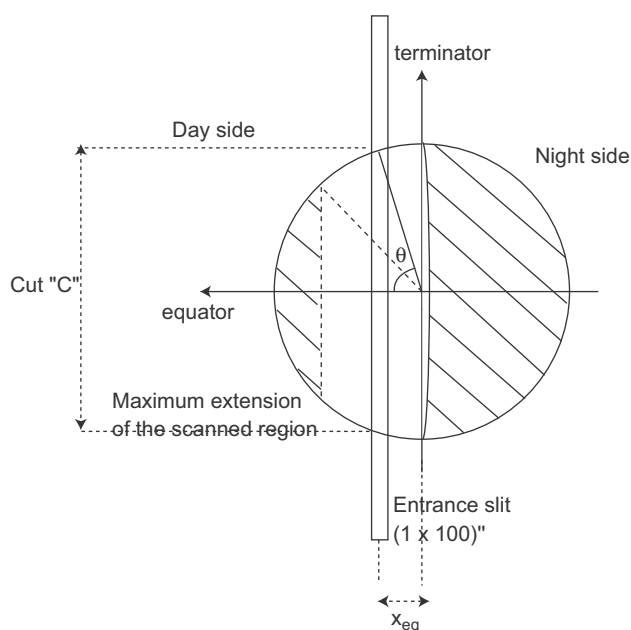


Fig. 2. Schematic review of notations used in this paper and illustration of the spatial coverage of Venus by our observations. The slanted lines indicate the region which is not covered by observations.  $\theta$  indicates the latitude and  $C$  the cut along the planet, through the entrance slit (in pixels). The maximum extension of the spatial coverage reaches  $\theta = 45^\circ$  on the planetary limb.

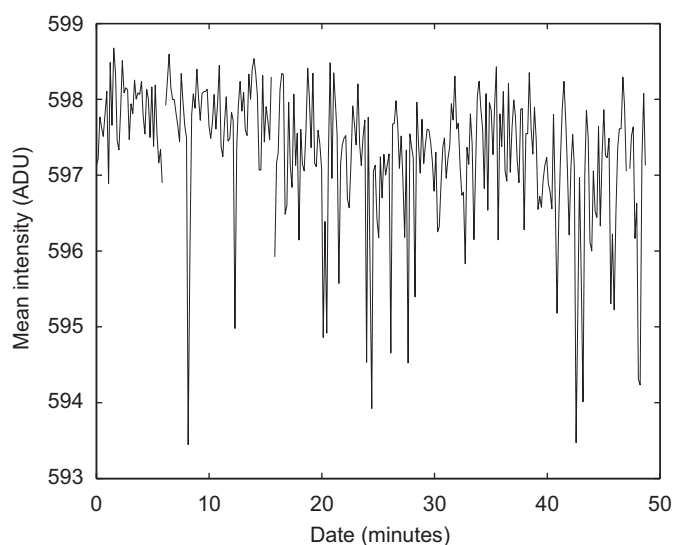


Fig. 3. Mean intensity measured on Earth's skylight background on each spectrum of the temporal series. The mean value is equal to 597.6 ADU, whereas the standard deviation of the points is equal to  $\Sigma = 58.16$  ADU.

surface is about  $0.5\text{m}^2$ , that the slit width is open at  $0.5\text{arcsec}$ , and that the global transmission is about 5% at  $5500\text{\AA}$ , we expect  $1156\text{ efficient photons s}^{-1}\text{arcsec}^{-2}$  on Venus. Since the total duration of the run is about 49 min and the spatial extension of the observed zone is about  $8\text{arcsec}$ , almost 6.1 min are dedicated per each  $1\text{-arcsec}$  position of the slit, i.e. for each Venus slab. Consequently, the total amount of photons per  $1\text{arcsec square}$  is almost  $4.23 \times 10^5$ , that is to

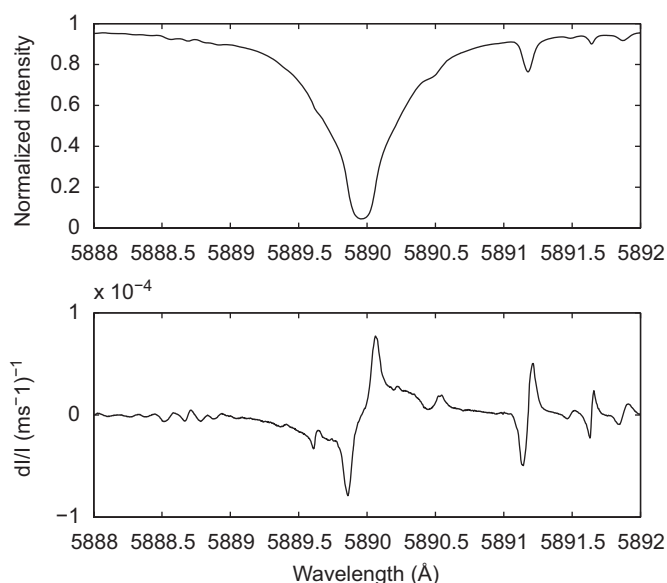


Fig. 4. Top: D2 sodium line on Sun spectrum as function of the wavelength (BASS 2000 database, <http://bass2000.obspm.fr>). Intensity has been normalised to 1. The Doppler sensitivity is related to the slope of the considered line. It reaches its maximum at the transmission level of 30%. Bottom: the slope of the upper figure, converted in meter per second. In average, the Doppler velocity sensitivity is about  $\langle \delta I/I \rangle = 0.5 \times 10^{-4}$  per  $\text{m s}^{-1}$  for a bandwidth of  $60\text{mÅ}$ .

say a signal to noise ratio  $\text{SNR} \simeq 650$ . Therefore, the expected  $1 - \sigma$  velocity sensitivity is about  $1/(650 \times 0.5 \times 10^{-4}) = 30.7\text{ m s}^{-1}$  per pixels of  $1\text{arcsec square}$ .

### 3. Data analysis

#### 3.1. Cleaning out raw spectra

Fig. 5 presents a typical raw spectrum obtained on Venus. Y-axis corresponds to spatial dimension, parallel to the terminator, and x-axis corresponds to spectral dimension. The spatial range corresponds to  $100\text{arcsec}$  and the total spectral range to  $6\text{\AA}$ . Since the entrance slit is much larger than the planetary diameter, most of the image is occupied by solar radiation scattered by Earth's atmosphere. The Doppler shift of the D2 sodium line between Venus and Earth atmosphere is clearly visible at image centre in Fig. 5 (left). Thinner lines crossing vertically the detector are telluric absorption lines. A slight distortion is visible across the field. This is a consequence of the optical design of the spectrometer. At first order, distortion parameters can be considered uniform across the field. We calculate them by fitting the Earth's D2 sodium line with a second order polynomial. The distortion is then rectified with a cubic spline interpolation algorithm. This effect is purely instrumental. Distortion can be considered constant through the observation run, so the fit has to be performed only once, on one image. The same correction algorithm is applied to all spectra.

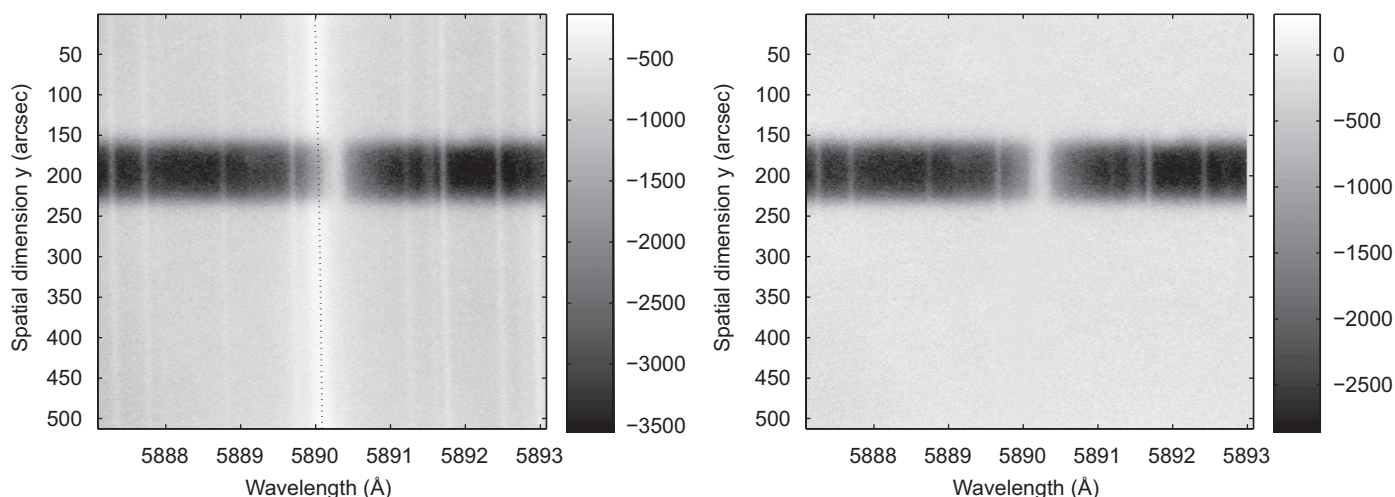


Fig. 5. Left: raw spectrum of Venus, centred on D2 sodium solar line. The  $y$ -axis corresponds the spatial dimension, while the  $x$ -axis squares with the spectral dimension. Venus corresponds to the dark region on the detector, with highest intensity, whereas the light background corresponds to the Earth's sky spectrum. The D2 line on Venus is clearly shifted with respect to the Earth's. The slight curvature across the whole image is estimated by fitting the D2 sodium line scattered by Earth's atmosphere with a second order polynomial (dot line). Right: clean spectrum. After straightening out the distortion, skylight sodium light has been averaged over the background, and subtracted to Venus. Thinner lines correspond to telluric absorption lines.

### 3.2. Positioning on the planetary disk

The main cause of uncertainty in processing the data comes from the positioning on the disk. Indeed, as the quick scan of the planet did not work, we have no direct measurement of the absolute position. The positioning is determined as a relative function of the initial pointing along the terminator. The spatial scale is determined using the spatial extension of Venus on first spectra, which covers 115 pixels, and fits the expected diameter of Venus upon the detector ( $21.76 \times 0.2 = 109$  pixel), taking into account the seeing effect. If we suppose that the slit slewed parallel to the terminator, the positioning upon the planet only depends on the ratio of the measured cut along the planet with respect to its size at terminator:

$$x_{\text{eq}} = \cos \theta \quad \text{with } \theta = C/D_{\text{venus}} \quad (1)$$

where  $x_{\text{eq}}$  indicates the  $x$ -coordinate along the planetary equator,  $\theta$  the latitude,  $C$  the extension of the planetary cut (pixels) and  $D_{\text{venus}}$  Venus measured diameter (pixels) (see Fig. 2). Note that this expression assumes that Venus was at quadrature (phase angle  $90^\circ$ ) and the central meridian is the terminator. The phase angle was  $84^\circ$  instead of  $90^\circ$ , yielding a difference of 1.1 arcsec, that is the spatial resolution by taking into account the seeing.

The spatial extension of Venus on the detector is determined after subtraction of Earth's skylight mean signal (Fig. 5). Then, the spectral image is projected along the  $y$ -axis, in order to get a smooth spatial profile. Venus' spatial dimension is arbitrarily defined as the region where the intensity exceeds the  $\frac{1}{2}$  of the maximum value, i.e. the full width at half maximum (FWHM) (see Fig. 6). We estimate the spatial extension at half maximum in order to minimise error due to seeing fluctuations, as illustrated in Fig. 6.

Plotting the FWHM as a function of time shows a slow drift, overlapped by a high frequency oscillation (Fig. 7). Such fluctuations are due to the bias introduced by rapid seeing (10-s interval from one image to another). The fit value used to calculate the position upon the planetary disk is obtained by a 3rd order polynomial. The standard deviation of the points with respect to their smoothed profile is about 2.46 pixels, which corresponds to 0.49 arcsec. This gives us the relative error bar of the slit position estimate  $x_{\text{eq}}$  on the disk (Fig. 2).

### 3.3. Doppler shift of D2 lines

Doppler maps are obtained by measuring the shift between the D2 sodium lines, scattered by Earth's and Venus' atmospheres. The shift must first be corrected from (i) Venus' centre motion with respect to observer and (ii) observer's motion with respect to the Sun. All these components are well known, and get subtracted with the help of ephemeris data (Fig. 8).

The Earth scattered solar D2 line intensity is averaged over all detector lines outside of Venus, to create a mean reference spectrum. On Venus, the 0.2-arcsec lines are coadded by groups of 5 in order to reach a 1-arcsec vertical resolution along the slit, thus improving the signal to noise ratio by a factor  $\sqrt{5}$ . The reference spectrum is then correlated to the spectrum measured on Venus, line by line; the Doppler shift corresponds to the position of maximum value of the cross correlation. Points are fitted with a 4th order polynomial, then, the maximum position is determined by calculating numerically the zeros of the derivative of the fitting function (Fig. 9). The fit accuracy is strongly dependent upon S/N; that is why we consider only the signal coming from Venus central region on the detector,

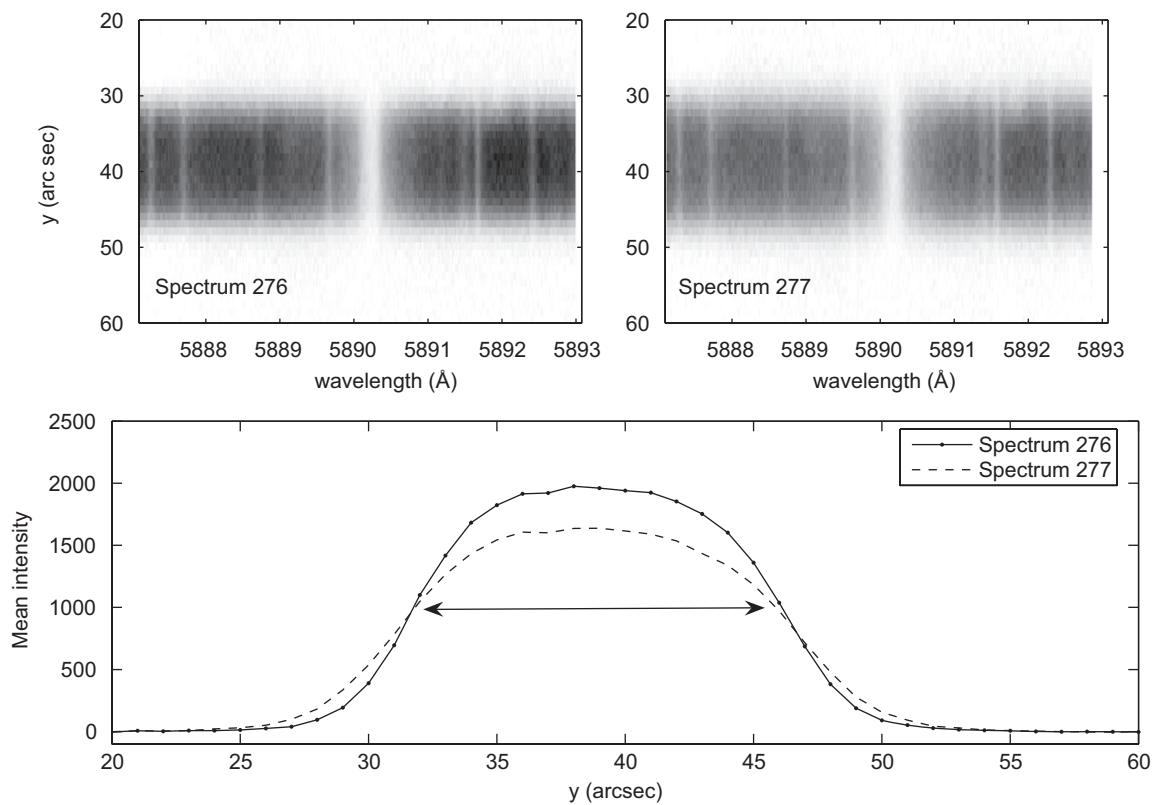


Fig. 6. Top: two consecutive spectra (labelled 276 and 277 among the 318 spectra temporal series), which have been acquired with an interval of 10 s. Bottom: projection of both spectra along the  $y$ -axis, in order to evaluate the spatial extension of the planet selected by the entrance slit. Width determination is the only method to locate the slit projection on Venus.

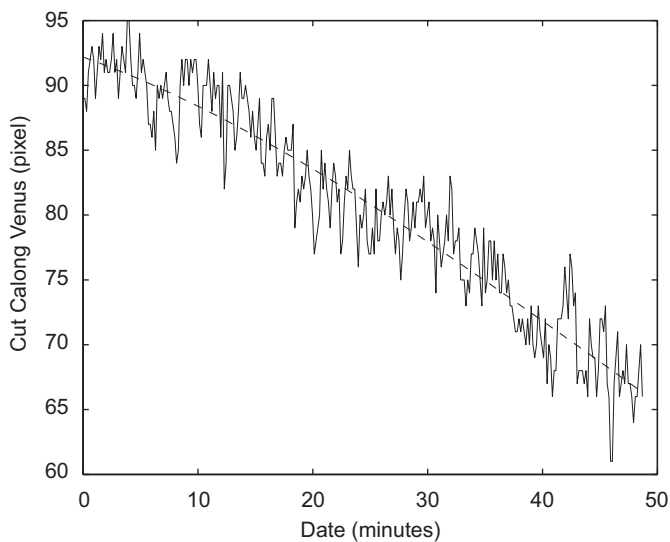


Fig. 7. Spatial extension estimate “C” as function of time, along the observation run. The cut extension has been calculated on full resolution images, in order to keep the original accuracy; 1 pixel corresponds to 0.2 arcsec. The extension is defined by the width at half maximum. The solid line represents the measurement of the spatial extension, while the dashed line represents the polynomial fitting of Venus cut. The standard deviation of points around the mean is equal to 2.46 pixels.

where amplitude is greater than half maximum amplitude, as for the cut estimate (previous section). In terms of angular size, it means to keep 16 arcsec instead of 21.8 arcsec along the diameter; in terms of latitude, it limits the map to  $\pm 45^\circ$ .

The global measurement of the Doppler shift is represented in a spatial-temporal diagram in Fig. 10, top left. Although the scan motion was perpendicular to terminator, we note that the upper edge of the planet is a straight line, whereas the bottom edge is curved. This is due to the fact that manual guiding was performed on the top of Venus image in the field (southern hemisphere). This guiding procedure and resulting vertical drift allowed us to reveal a spectral artifact probably due to the missing calibration procedures we referred to in Sections 2 and 2.3. This spectral artifact is visible in Fig. 10, top left frame, as a white horizontal band between  $y = 40$  and 45 arcsec. We decided to pursue the analysis by trying to correct it the following way. First, we coadded all the lines to assess the mean variation of the Doppler integrated over slit height. This mean variation is shown in Fig. 10, bottom. It shows qualitatively that the spectral shift between Earth’s solar D2 and Venus’ solar D2 decreases as the slit moves away from terminator. This average decrease is then fitted to a

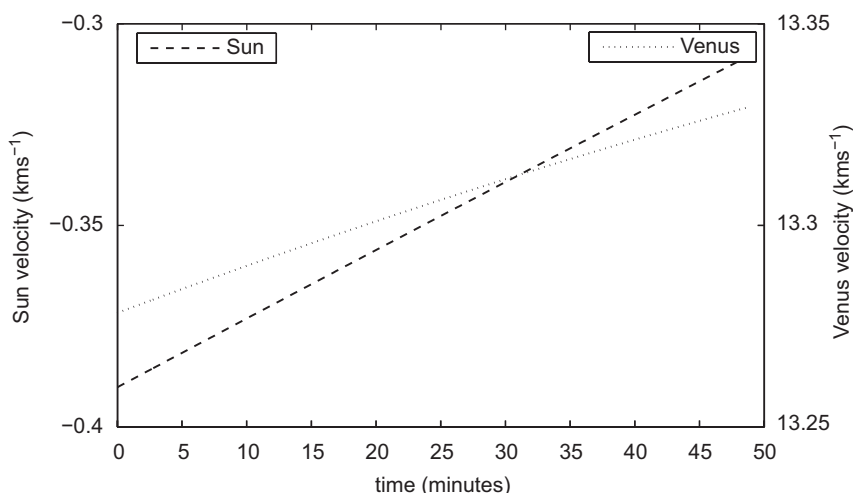


Fig. 8. Relative velocities with respect to Teide Observatory between 13:06:52 and 13:55:34 h (UT) on November, 7th 2007. Initial date squares with 13:06:00 h, velocities are expressed in  $\text{km s}^{-1}$ . Left y-axis indicates Sun relative velocity, which mean amplitude is about  $-0.35 \text{ km s}^{-1}$ . Right y-axis indicates Venus relative velocity, which mean is about  $+13.3 \text{ km s}^{-1}$ . Consequently, the mean Doppler shift between D2 sodium line scattered by Venus' and Earth' atmospheres is equal to  $+13.65 \text{ km s}^{-1}$  ([www.imcce.fr](http://www.imcce.fr)).

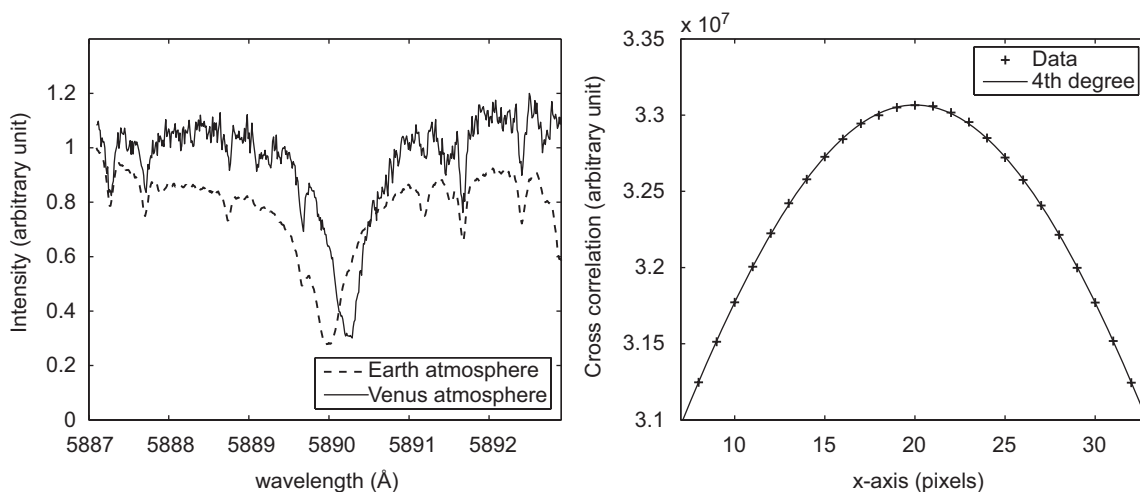


Fig. 9. Left: reference mean spectrum (dashed line) and Venus spectrum as a function of the wavelength (full line). Reference spectrum is calculated for each spectrum by averaging all the skylight spectrum. Venus spectrum is obtained on a 1 arcsec spatial resolution spectrum, and correspond to the planetary equator. Both spectrum have been normalised with respect to their maximum value and Venus spectrum has been offset, only for graphical reasons. Right: 4th order polynomial fit of the maximum of the cross correlation between Venus and reference spectra. The maximum position is equal to 20.51 pixels.

weighted moving average in order to flatten the Doppler surface, with respect to time, prior to the kinematical fit described in Section 4. Second, the temporal mean of this diagram, shown in Fig. 10, right frame, has been subtracted to the main data frame in order to remove the artifact. The result is shown in Fig. 11.

## 4. Results

### 4.1. Working with relative velocities

Strong discrepancies of up to several tens of  $\text{m s}^{-1}$  have been commonly met with tentatives of making absolute

radial velocity measures using visible lines. This has been discussed in the case of Venus wind measurements in Young et al. (1979) and Widemann et al. (2007, 2008). These authors concluded for the need of a reference point on Venus used as a relative velocity reference, and they used this point to perform differential velocity measurements on the disk. The 0 velocity is fixed at the planetary coordinates ( $\theta = 0^\circ, \alpha = 5^\circ$ ), where  $\theta$  and  $\alpha$  indicate the latitude and longitude.

The radial velocity map is shown in Fig. 12. The maximum velocity difference on the whole map reaches almost  $300 \text{ m s}^{-1}$ , while the mean amplitude of the variation of velocity across the planet is about  $200 \text{ m s}^{-1}$ .

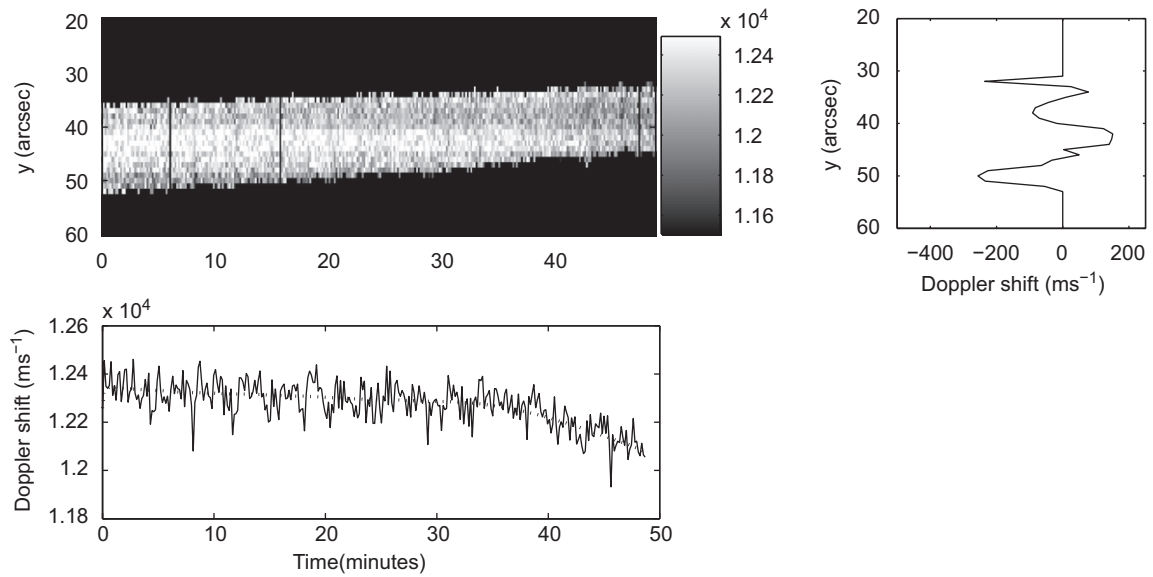


Fig. 10. Top left: Doppler shift diagram as a function of time ( $x$ -axis) and space ( $y$ -axis). Doppler shift is expressed in  $10^4 \text{ms}^{-1}$ . Bottom left: mean Doppler shift with time. Top right: mean Doppler shift with spatial dimension. The dashed line on the bottom left plot indicates the fitted estimate obtained by a weighted moving average, which has been used to characterise the vertical distortion of the Doppler “surface” plotted in bottom right figure.

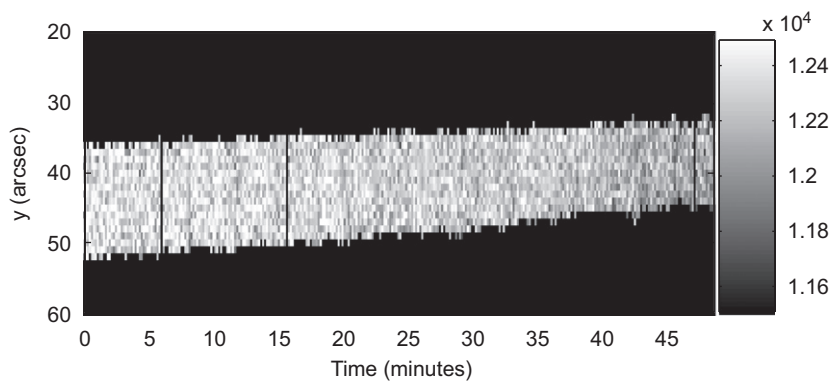


Fig. 11. Clean Doppler diagram, obtained after subtraction of the spurious distorted “surface” enlightened in the raw diagram (Fig. 10).

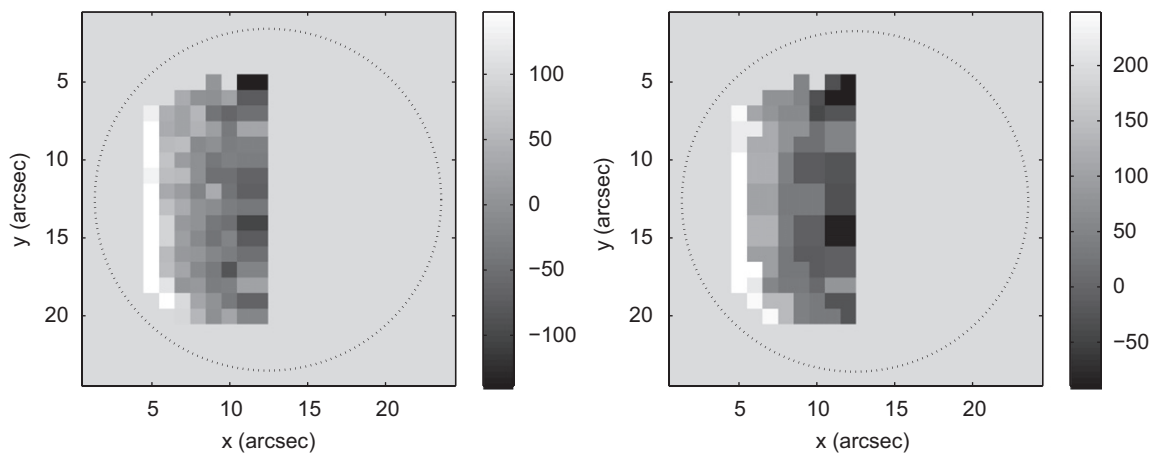


Fig. 12. Left: relative velocity map obtained after summation of Doppler shift within 1-arcsec intervals. The dot line circle indicates the planetary diameter. The maximum latitude extension reaches  $\pm 45^\circ$ , while the maximum longitude reaches 55 at pixels (5, 7) and (5, 17). Right: the same Doppler map where pixels have been averaged within a regular latitude–longitude grid, spaced by  $10^\circ$ . Latitude range is  $[-45^\circ, 45^\circ]$  while longitude range is  $[0^\circ, 55^\circ]$ .

Table 2  
Standard deviation  $\Sigma$  of velocity in each column of the Venus map

Abscissa $x$	(12, 11)	10	9	8	7	6	5
$\Sigma$ ( $\text{m s}^{-1}$ )	42.96	27.60	25.06	23.93	30.27	33.00	34.72
Number of spectra	30	31	40	48	56	67	43

The mean standard deviation value is equal to  $31 \text{ m s}^{-1}$ . The third line indicates the number of spectra averaged in order to build each column. We have averaged columns 11 and 12 because column 11 alone have only five spectra, which affect the global noise level. The standard deviation increases in columns 5–7 despite a major number of averaged spectra, because of the wind velocity strong variation in these columns.

A rough estimate of the actual mean noise level can be obtained by measuring the standard deviation  $\Sigma$  of each “column of pixels” on Venus figure. The mean value of the dispersion of points along a column is equal to  $31 \text{ m s}^{-1}$  (see Table 2). Note that the higher noise level, which is observed in column of abscissa  $x = [5, 6]$ , is due to a geometrical effect. Indeed, the wind velocity on Venus varies more strongly in columns far from the terminator, because a wide range of longitude is explored, what increases the standard deviation of the considered column. This fact makes the mean standard deviation value appear as a slightly pessimistic estimate of the actual mean noise level per pixel. Nevertheless, its value, about  $31 \text{ m s}^{-1}$ , almost squares with the theoretical performance ( $30.7 \text{ m s}^{-1}$ ) presented in Section 2.3, what shows that our estimate of the noise level is correct.

#### 4.2. Fit of Doppler winds to zonal circulation

Doppler blueshift between Venus’ atmosphere and the Sun is maximum along the terminator, whereas Doppler redshift between Earth and Venus is maximum along the planetary limb. By supposing a purely zonal wind, the isotach corresponding to radial velocity  $v_{\text{rad}} = 0$  is the meridian defined by the bisecting angle between sub-earth and sub-solar longitudes. Moreover, a correction has been introduced by Young et al. (1979), taking into account the solar apparent diameter and its rotation seen from Venus (42 arcmin), so-called *Young effect* (see also Widemann et al., 2008).

The consequence is an increase of the apparent Doppler shift for the observer, along the terminator at mid and high latitudes ( $\pm 45^\circ$ ). The typical amplitude of the wind increase reaches almost  $30 \text{ m s}^{-1}$  for a  $100 \text{ m s}^{-1}$  zonal wind, and therefore must be arbitrarily corrected in a kinematical fit to a pure zonal regime.

The algorithm used to extract the velocity amplitude from the radial velocity map has been adapted from Widemann et al. (2007). The zonal circulation at cloud top level is characterised by a latitudinal dependency and wind decrease in the polar regions. Recently reanalysed Pioneer Venus UV data (Limaye, 2007) and SSI Galileo imaging (Peralta et al., 2007) indicate a generally

uniform velocity between latitude  $\pm 50^\circ$  with a best fit to a constant angular velocity at higher latitudes, in accordance with winds measured from cloud tracking by both VIRTIS-M and VMC (Markiewicz et al., 2007; Piccioni et al., 2007). Both types of zonal wind regimes dependency have been applied to fit our data using classical least-square algorithm.

For a uniform, solid body circulation, the wind velocity is estimated at  $2 - \sigma$  at  $151 \pm 16 \text{ m s}^{-1}$ , with reduced  $\chi^2 = 1.69$ . On the other hand, with a cosine latitudinal dependance, the zonal wind velocity is estimated at  $146 \pm 17 \text{ m s}^{-1}$ , with reduced  $\chi^2 = 1.85$ . The close results between the two approaches is due to the fact that our observations do not explore (with good SNR) Venus wind map at latitude higher than  $45^\circ$ . Under this latitude, the difference between both models is not very significant. It has to be noticed that uncertainties on the wind global velocity ( $16\text{--}17 \text{ m s}^{-1}$ ) is larger than what would be expected from local noise level. Indeed, with a local noise level of  $31 \text{ m s}^{-1}$  per 1 arcsec square pixel on about 128 pixels, the global noise level by integrating all Venus’ pixels would decrease to  $31/\sqrt{128} = 2.7 \text{ m s}^{-1}$ . This lower performance is due to three facts. First, the sensitivity of Doppler measurements to velocity is not uniform on the planet (isotachs are functions of longitude, e.g. Widemann et al., 2007). Second, the real velocity field might not be uniform as supposed inside the model used to fit the data. At last, the previously exposed uncertainty about the positioning introduces a bias in the global fit.

Our result is compatible with Doppler spectroscopy measurements of Widemann et al. (2007), where the wind amplitude is estimated in a  $[90, 150] \text{ m s}^{-1}$  velocity range. However, this result represents an upper value with respect to VEx results of Markiewicz et al. (2007), who have obtained a mean value zonal wind of  $95 \text{ m s}^{-1}$  between latitudes 10N and 40S, using cloud tracking method. Two reasons may explain the discrepancy between our results and those of Markiewicz et al. (2007). First, it could be a consequence of the uncertainty on the positioning, what would implies a  $60\text{-m s}^{-1}$  bias in global velocity estimate. Second, it might point out the fact that cloud tracking and Doppler spectrometry are two distinct approaches to measure the wind velocity. With cloud tracking, one measure the cloud feature motion, while Doppler spectrometry measures the cloud particle motion, which may differ.

## 5. Conclusions and prospects

The goal of our observations was to evaluate the ability of the MTR/THEMIS solar telescope in order to measure velocity wind by Doppler spectroscopy in the visible range. Despite cloudy weather, and consequently a very short run (49 min), we obtain a promising instrumental performance: the mean noise level on the velocity map is about  $31 \text{ m s}^{-1}$  per 1-arcsec pixel, which corresponds to the expectations. As regards the wind velocity field, it has been estimated at

$149 \pm 16 \text{ m s}^{-1}$ , what represents a quiet excessive value with respect to other observations. We have given two possible explanations. First, it could come from a global bias introduced by the observation conditions, in particular to the lack of quick scan, which has made the positioning upon the planetary disk noisy. Also, it might be due to the fact that cloud tracking and Doppler measurements represent different approaches to wind velocity estimate. Part of this spurious velocity which has been seen in Fig. 10 would be skipped out with the use of the tip-tilt guiding system and by optimising the instrumental configuration. By supposing the same local noise level ( $31 \text{ m s}^{-1}$ ) and by choosing Fraunhofer lines with a better sensitivity to Doppler shifts, it would be possible to reach a noise level around  $10 \text{ m s}^{-1}$  per 1 arcsec square in few hour observation run and to reach a global wind measurement accuracy of about several  $\text{m s}^{-1}$ .

These encouraging performances have motivated a new observation campaign, which is planned for mid spring 2008. Tip-tilt guiding will be used. Venus will present a shorter apparent diameter (10 arcsec) and a greater phase (90%). Four deep solar lines will be used to measure velocity fields (Fe I, Mg, D1 and D2 Na), in order to gain a factor 2 in the SNR. Moreover, the Doppler shift of  $\text{CO}_2$  line ( $v_3$  band,  $8680 \text{ \AA}$ ) will be studied in order to probe 7 km higher. Future observations will be of major interest because at short elongation Venus is practically unobser-

vable with classical night telescopes, whereas VEx is still orbiting around Venus.

## References

- Drossart, P., Piccioni, G., Adriani, A., et al., 2007. Scientific goals for the observation of Venus by VIRTIS on ESA/Venus Express mission. *Planet. Space Sci.* 55, 1653.
- Limaye, S.S., 2007. Venus atmospheric circulation: known and unknown. *J. Geophys. Res.* 112, 4.
- Markiewicz, W.J., Titov, D.V., Limaye, S.S., et al., 2007. Morphology and dynamics of the upper cloud layer of Venus. *Nature* 450 (7170), 633–636.
- Mein, P., Rayrole, J., 1985. Themis solar telescope. *Vistas Astron.* 28 (2), 567–569.
- Peralta, J., Hueso, R., Schez-Lavega, A., 2007. A reanalysis of Venus winds at two cloud levels from Galileo SSI images. *Icarus* 190 (2), 469–477.
- Piccioni, G., Drossart, P., Sanchez-Lavega, A., et al., 2007. A dynamic upper atmosphere of Venus as revealed by VIRTIS on Venus Express. *Nature* 450(7170), 641–645.
- Rayrole, J., Mein, P., 1994. THEMIS telescope: prospects in high resolution magnetic field observations. *IAU Colloquium No. 141*, p. 170.
- Widemann, T., Lellouch, E., Campargue, A., 2007. New wind measurements in Venus lower mesosphere from visible spectroscopy. *Planet. Space Sci.* 55 (12), 1741–1756.
- Widemann, T., Lellouch, E., Donati, J.-F., 2008. Venus Doppler winds at cloud tops observed with Espadons at CFHT, this issue, doi:10.1016/j.pss.2008.07.005.
- Young, A.T., Schorn, R.A., Young, L.D.G., Crisp, D., 1979. Spectroscopic observations of winds on Venus. I—Technique and data reduction. *Icarus* 38, 435–450.